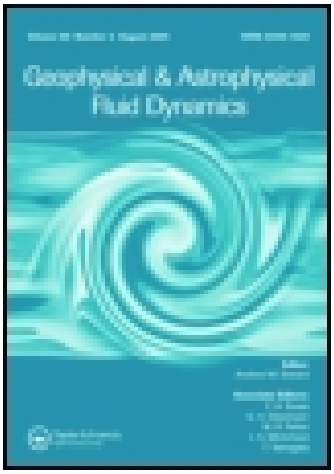

Geophysical & Astrophysical Fluid Dynamics
Publication details, including instructions for authors and subscription information:
http://www.tandfonline.com/loi/ggaf20

# The influence of a side wall on rotating flow over bottom topography

R. W. Griffiths [a] & P. F. Linden [b]

[a] Department of Applied Mathematics and Theoretical Physics , University of Cambridge , Silver Street, Cambridge CB3 9EW, U.K

[b] Research School of Earth Sciences, Australian National University , P.O. Box 4, Canberra 2601, Australia

Published online: 18 Aug 2006.

To cite this article: R. W. Griffiths & P. F. Linden (1983) The influence of a side wall on rotating flow over bottom topography, Geophysical & Astrophysical Fluid Dynamics, 27:1-2, 1-33

To link to this article: http://dx.doi.org/10.1080/03091928308210119

*Geophys. Astrophys. Fluid Dynamics*, 1983, Vol. 27, pp. 1–33
0309-1929/83/2702-0001 $18.50/0

Printed in Great Britain



# The Influence of a Side Wall on Rotating Flow over Bottom Topography

R. W. GRIFFITHS† and P. F. LINDEN

*Department of Applied Mathematics and Theoretical Physics, University of Cambridge, Silver Street, Cambridge CB3 9EW, U.K.*

(*Received March 10, 1983; in final form July 4, 1983*)

We describe laboratory observations of the flow of a homogeneous fluid over three-dimensional obstacles that are towed along the bottom of one vertical wall of a wide rotating channel. The behaviour of the viscous–inertial flow, for a given direction of rotation, depends strongly upon whether the wall is on the right- or left-hand side when looking downstream (in the direction of flow relative to the obstacle). There are a number of flow regimes, with a blocked region occurring above the topography at low Rossby numbers when the wall is on the right of the flow (for anticlockwise rotation), but a large blocked region developing downstream of the obstacle when the wall is on the left. Blocking on the left-hand wall occurs at larger Rossby numbers than on the right-hand wall, contrary to theoretical predictions for slowly varying topography or linearised disturbances. When the influence of viscosity is sufficiently small the blocked region against a left-hand wall gives way to a train of cyclonic eddies. No wake is seen when the wall is on the right of the flow and there are no anticyclonic eddies. At large Rossby numbers the disturbance takes the form of a system of standing inertial lee waves.

## 1. INTRODUCTION

The steady flow of homogeneous fluid over isolated topography (such as a truncated cylinder or hemisphere) in a rotating system has

†Present address: Research School of Earth Sciences, Australian National University, P.O. Box 4, Canberra 2601, Australia.

been extensively investigated in both numerical and laboratory experiments. At finite Rossby numbers, inertial effects cause this flow to possess a left–right asymmetry when looking in the direction of the mean velocity (e.g. Ingersoll, 1969; Huppert, 1975; and the review by Baines and Davies, 1980). This observation suggests that, when a vertical wall is present near the obstacle, the structure of the resulting flow will (for a given sign of rotation) depend upon whether the wall is on its right- or left-hand side.

The influence of two side walls upon the flow over a two-dimensional obstacle extending between the walls of a rotating channel or annulus has been observed in laboratory experiments for both shallow obstacles (Boyer, 1971a, b) and obstacle heights comparable to the fluid depth (Maxworthy, 1977). Huppert and Stern (1974a) have analysed the influence of the walls on such a flow in order to predict the net horizontal displacement of streamlines far downstream. Maxworthy's experiments in an annular channel reveal a system of inertial lee waves downstream of the ridge when the Rossby number is so large that the fluid passes almost directly over the ridge. For smaller Rossby numbers and large obstacle heights a large blocked region develops downstream of the ridge against the left-hand side of the channel. No streamlines originating upstream enter the blocked region—they are first deflected to the left over the ridge and are then deflected far to the right, away from the left wall near the downstream side of the obstacle. At still smaller Rossby numbers the flow is completely blocked, with no streamlines passing over the ridge. Huppert and Stern (1974b) present a linearised analysis for the (stratified) flow over an obstacle of any cross-stream profile in such a channel and show that blocking will occur first on the right-hand wall (with anticlockwise rotation) directly over the obstacle. The observed blocking on the left wall is not predicted.

Apart from the above observations of the flow downstream from two-dimensional obstacles, little attention has been paid to the structure of flow *downstream* of submerged obstacles in a rotating system. Most experiments with shallow, isolated topography (e.g. Vaziri and Boyer, 1971; Hide and Ibbetson, 1966; Davies, 1972) appear to indicate a smooth transition between a region of largest velocity perturbations at the obstacle and an undisturbed parallel flow far downstream. Boyer (1970), and Boyer and Davies (1982) however, have made a detailed investigation of the flow around

vertical cylinders that extend throughout the depth of the fluid. In this case rotation produces an asymmetry in the wake of the cylinder, and eddy shedding occurs when the Reynolds number is greater than a critical value, a value that for a given cylinder aspect ratio increases with decreasing Rossby number.

Here we describe the flow that is produced when a three-dimensional obstacle, with height, length and width all comparable to the fluid depth, is towed at a constant velocity along a wide rotating channel. The obstacle is placed against one wall and the bottom of the channel. We have concentrated on obstacle heights $\eta_0$ that are a large fraction of the fluid depth $H$, $\eta_0/H \geqq \frac{1}{4}$. This range of $\eta_0$ is of direct relevance to coastal regions where oceanic flow over bottom topography can be influenced by the presence of the coastal boundary, though the laboratory model does not include a realistic variation of fluid depth near the boundary.

The flow is found to be very different depending on the direction of motion of the obstacle or, equivalently, the sign of rotation, or whether the obstacle is against the left- or right-hand wall. When the obstacle is adjacent to a wall on the right-hand side of the flow (looking downstream and with anticlockwise rotation) the topography has very little downstream influence apart from a system of large amplitude standing inertial lee waves at larger Rossby numbers, while there is always a large downstream influence when the wall is on the left of the flow. Blocking occurs at sufficiently low Rossby numbers in both cases but the critical value is larger when the wall is on the left. In the case of a wall on the right of the flow, blocking corresponds to the formation of a Taylor column above the obstacle but for a left-hand wall the blocked region extends far downstream. At intermediate Rossby numbers unstable waves sometimes appear on the outer edge of the downstream blocked region and give rise to cyclonic eddies in the shear layer. At slightly larger Rossby numbers, cyclonic eddies can be shed immediately behind the obstacle and these tend to break up the blocked region. The flow around a vertical half-cylinder against one wall and extending throughout the fluid depth is also described. This flow again involves a large, almost stagnant region downstream at small Rossby numbers when the wall is on the left of the flow, and unsteady shedding of eddies at larger Rossby numbers.

## 2. FLOW OVER SLOWLY VARYING OBSTACLES

Some aspects of the behaviour of flow over an obstacle near a vertical wall are usefully obtained from an analysis such as that presented by Huppert and Stern (1974b). These authors considered both linearised stratified flow over three-dimensional obstacles in a rotating channel and the inviscid homogeneous flow along a channel whose depth varies slowly in the downstream direction. In both cases a stagnation point appeared on the right-hand wall (looking downstream when the system is rotating anticlockwise) for a critical relationship between the Rossby number and the depth variation (or obstacle height). We present a similar analysis here to show clearly the conditions for blocking when the channel is very much wider than the obstacle, and the dependence of the critical condition upon the obstacle geometry.

We consider a fluid of depth $H$ flowing in the $y$ direction along a channel of width $L$ which rotates with angular velocity $\Omega$. As shown in Figure 1 the channel walls are at $x=0, L$ and the obstacle has a height $\eta(x, y)$, which we assume to be a maximum $\eta_0$ at the wall $x=0$. A cross-stream scale for the obstacle is $l$ and the fluid far upstream has a uniform velocity $V$. Although a full solution for the velocity and pressure fields can readily be obtained from the appropriate linearised equations, it will be seen that the most interesting aspects of the observed behaviour in the experiments are essentially non-linear and not predicted by such a solution. The simplest possible non-linear analysis—but assuming the obstacle to be slowly varying in the downstream direction—is therefore given. Apart from the assumption of a slowly varying topography, no linearisation is made so that the velocity perturbations and obstacle height may be large compared to the upstream velocity and depth, respectively.

Since the upstream depth and velocity are uniform the fluid has a uniform potential vorticity $f/H$, where $f=2\Omega$, and this must be conserved by fluid columns as they pass the obstacle. Hence

$$\frac{f+v_x-u_y}{H-\eta}=\frac{f}{H}. \tag{2.1}$$

Because the topography is slowly varying in the $y$ direction the term

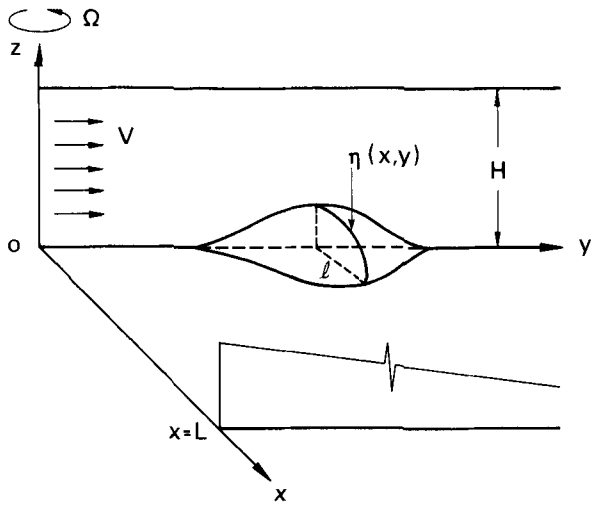


FIGURE 1 The theoretical and experimental system.

$u_y$ in (2.1) can be neglected. Writing $\eta=\eta_0 h(x/l, y/l)$, with $0\leqq h\leqq 1$, the relative vorticity becomes

$$v_x=-\frac{f\eta_0}{H}h\left(\frac{x}{l},\frac{y}{l}\right). \tag{2.2}$$

Integration of (2.2) gives the downstream velocity perturbation

$$v(x,y)=v_0(y)-\frac{f\eta_0}{H}\int_0^{x/l}h\left(\frac{x}{l},\frac{y}{l}\right)d\left(\frac{x}{l}\right), \tag{2.3}$$

where $v_0(y)$ is the velocity perturbation on the wall $x=0$.

The value of $v_0$ is found from the continuity equation

$$VHL=\int_0^L (V+v)(H-\eta)\,dx. \tag{2.4}$$

After scaling all horizontal velocities by $fl$, all horizontal lengths

$(x, y, L)$ by the obstacle width $l$, and the obstacle height by the total fluid depth $H$, the dimensionless perturbation is

$$v_0 = \frac{\eta_0 \left[ Ro \int_0^L h\,dx + \int_0^L \int_0^x h\,dx^2 - \eta_0 \int_0^L h \left( \int_0^x h\,dx \right) dx \right]}{\left[ L - \eta_0 \int_0^L h\,dx \right]}, \tag{2.5}$$

where $Ro = V/fl$ is the dimensionless velocity and a Rossby number for the flow. Defining the cross-sectional area of the obstacle in the form

$$a(x, y) = \int_0^x h\,dx, \quad A = a(L, y),$$

the dimensionless form of (2.3) gives the total downstream perturbation as

$$v(x, y) = v_0 - \eta_0 a, \tag{2.6}$$

where (2.5) becomes

$$v_0(y) = \frac{\eta_0 \left[ Ro\,A + \int_0^L a\,dx - \eta_0 \int_0^L ha\,dx \right]}{[L - \eta_0 A]}.$$

Assuming that there are no closed streamlines anywhere in the flow, (2.6) implies that $v = 0$ whenever $a = 0$. Hence there is no perturbation to the uniform flow upstream or downstream of the obstacle. Furthermore, for topography that is everywhere positive the velocity perturbation is always largest (most positive) at the wall $x = 0$ and smallest (perhaps negative) at $x = L$. This conclusion is independent of the distribution of $h(x, y)$ and independent of the sign of the dimensionless velocity $Ro$ (which is determined by the signs of $V$ and $\Omega$). Since the maximum and minimum values of $v$ always occur at the walls of the channel, where $u = 0$ as well, there is a stagnation point in the flow when the total downstream velocity

$Ro+v$ vanishes. This occurs when

$$\frac{Ro}{\eta_0}=\left(1-\frac{\eta_0}{L}A\right)a-\frac{1}{L}\int_0^L a\,dx+\frac{\eta_0}{L}\int_0^L ha\,dx. \tag{2.7}$$

For very wide channels ($L\gg 1$), or when the wall at $y=L$ is removed to infinity, the condition (2.7) reduces to

$$\frac{Ro}{\eta_0}=a-\frac{1}{L}\int_0^L a\,dx. \tag{2.8}$$

We have seen that the maximum and minimum perturbations $v$ occur on the walls and this implies that, as the Rossby number is reduced, stagnation must occur first at the side of the channel. At $x=0$ (2.8) becomes

$$\frac{Ro}{\eta_0}=-\frac{1}{L}\int_0^L a\,dx, \quad L\gg 1, \tag{2.9}$$

the negative value indicating that either the velocity $V$ or the rotation $\Omega$ must be negative for stagnation to occur at $x=0$. (An equivalent condition can be obtained from (2.8) for blocking at $y=L$ in a channel of finite width, and this yields a positive Rossby number.) Thus blocking is predicted to be possible only when the wall is on the right-hand side of the flow. The same qualitative conclusion is drawn from a linearised Fourier series analysis [similar to that presented by Huppert and Stern, (1974b)] of the flow over more general obstacle shapes, allowing for rapid downstream variations of the obstacle height.

For an obstacle confined to within $0\leqq x\leqq 1$, (2.9) implies that the flow is blocked for Rossby numbers satisfying

$$|Ro|\leqq\eta_0\int_0^1 h\,dx, \tag{2.10}$$

where the right-hand side is to be evaluated at the value of $y$ at which the obstacle presents its maximum cross-sectional area. This result is equivalent to that obtained by Huppert (1975) for axisymmetric isolated obstacles, and corresponds to the formation of a Taylor column above the topography.

## 3. THE EXPERIMENTAL APPARATUS

Solid obstacles of spherical, cylindrical and triangular shape were towed along the length of a rectangular channel 120 cm long and 30 cm wide. The channel was mounted on a direct-drive turntable with a vertical axis of rotation and whose direction of rotation could be reversed. Three different obstacle shapes were employed, each having two perpendicular planar surfaces which fitted flush against the bottom and one wall of the channel. One obstacle was a quarter-sphere of radius 5.0 cm and another was a truncated half-cylinder of radius and length 5.0 cm with its axis aligned to the vertical so that it presented a horizontal semi-circular upper surface. Thus both of these shapes have their width $l$, length $d$ and height $\eta_0$ identical. The third obstacle was a 15 cm long ridge with the cross-section in the form of an isosceles triangle with base and altitude measuring 5 cm. The triangular end was placed against the side wall and the base against the floor of the channel. This obstacle represented a sharp-crested ridge of height $\eta_0$ and downstream scale $d$ both equal to 5 cm, projecting a distance $l = 15$ cm perpendicular to the wall.

In order to keep the obstacles flush against the side wall this wall was an internal partition of the channel, as shown in Figure 2. The obstacles were attached, by an arm passing through a 0.5 cm gap below the internal wall and through the narrow space between the two walls, to a carriage that was towed with a constant velocity along the top of the wall. Any flow of fluid through the gap beneath the wall is expected to have an insignificant effect on the flow in the channel since the quarter-sphere and vertical half-cylinder extend ten times farther from the bottom.

In order to vary the ratio of obstacle height $\eta_0$ and width $l$ to the total fluid depth $H$, the latter was adjusted between 5 cm and 20 cm. Observations were made for the ratios $\eta_0/H = \frac{1}{4}$, $\frac{1}{2}$ and 1 for each obstacle shape. The influence of viscosity, expressed in terms of the Ekman number $E = \nu/2\Omega H^2$, where $\nu$ is the kinematic viscosity of the water, varied due to adjustments of both $H$ and $\Omega$, the rotation rate lying in the range $0.1 < \Omega < 1.5\ \mathrm{rad\,s^{-1}}$. For a given Ekman number and obstacle height $\eta_0/H$ the value of the Rossby number, $Ro = V/2\Omega l$, was then selected by adjusting the towing speed within the range $0.15 < V < 3.2\ \mathrm{cm\,s^{-1}}$.

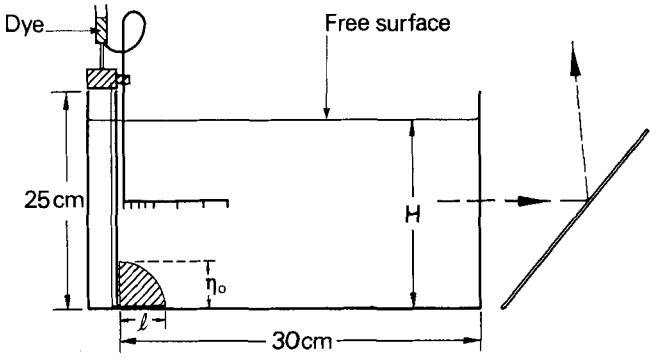


FIGURE 2 The laboratory apparatus, showing the towing mechanism and dye injection tubes as seen when looking along the channel. Dye is emitted from the (horizontal) ends of the small tubes, which are placed ~10 cm ahead of the obstacle. The obstacle is towed at a constant speed in the direction out of the page.

The flow around the obstacles was made visible by continuously injecting dye from a horizontal line of small tubes. This was usually positioned ~10 cm ahead of the moving obstacle and at any desired depth. Because the velocities used in some experiments were very small it was necessary to add sugar to the water in the channel to make the dye as close as possible to neutrally buoyant. (Sugar was used in preference to salt in order to reduce the growth rate of double-diffusive instabilities.) It was also necessary to seal the top of the channel as much as possible with a Perspex lid in order to reduce motions driven by evaporative convection and wind stress at the free surface. The dye lines then marked streamlines until they became distorted due to convective instabilities. They were photographed in plan view by a camera mounted in the rotating frame of reference and above the channel. The same photograph recorded a side-view of the dye lines, showing their vertical excursions, when a mirror was placed at roughtly 45° beside the channel, as shown in Figure 2, or inside the channel against the wall opposite the obstacle.

Since a change in the direction of motion of the obstacle is equivalent to a change in the direction of rotation of the system the obstacle was, for convenience in the construction of the towing mechanism, usually towed in the same direction—with the wall on

its right when looking in the direction of motion—and the flow observed for both directions of rotation. Thus the wall was usually on the left-hand side of the flow over the obstacle when looking downstream. When the rotation is clockwise (negative), the resulting flow is identical to that over an obstacle against a right-hand wall (looking downstream) in a system rotating in the anticlockwise (positive) direction.

## 4. EXPERIMENTAL RESULTS

### 4.1. Flow over submerged obstacles for clockwise rotation

The structure of the flow about the quarter-sphere and vertical half-cylinder will be described first for the case of clockwise (negative) rotation. On Figures 3(a) and (b) are shown two photographs of the flow over the quarter-sphere for a fluid depth that gives $\eta_0/H = l/H = \frac{1}{4}$ when the rotation is clockwise. In each case the obstacle is moving from left to right. In the first photograph [Figure 3(a)] the Rossby number is $Ro = 0.03$ and the flow consists of a region of closed streamlines over the obstacle and adjacent to the wall, about which all streamlines originating upstream are deflected. At such low Rossby numbers these streamlines flow roughly around the contours of constant depth (there being very little flow over the obstacle except for the innermost streamline) and return to their initial distance from the wall behind the obstacle. The blocked region into which upstream dye does not penetrate is a Taylor column that is influenced by a finite Rossby number and by the viscous retardation produced by the obstacle itself and by the relative motion of the wall. Fluid within the blocked region undergoes a slow anticyclonic (anticlockwise) motion but is almost stagnant. The topography has very little downstream influence.

The second photograph [Figure 3(b)] reveals another flow regime. This time the Rossby number is larger, $Ro = 0.11$ and the disturbance to the uniform flow consists entirely of inertial lee waves above and downstream of the topography. For both photographs the dyed streamlines originate at the depth of the top of the obstacle (5 cm above the bottom).

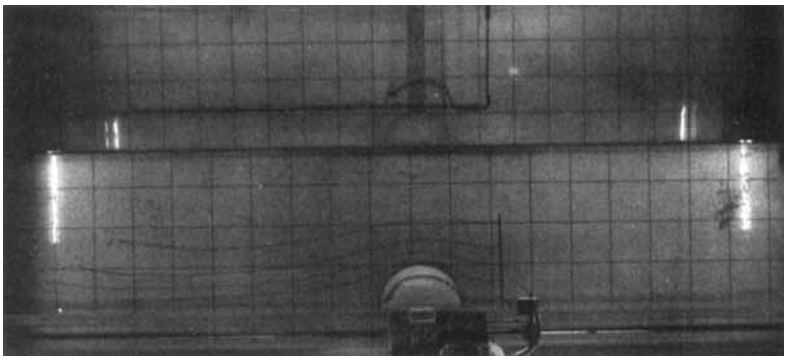

3(a)

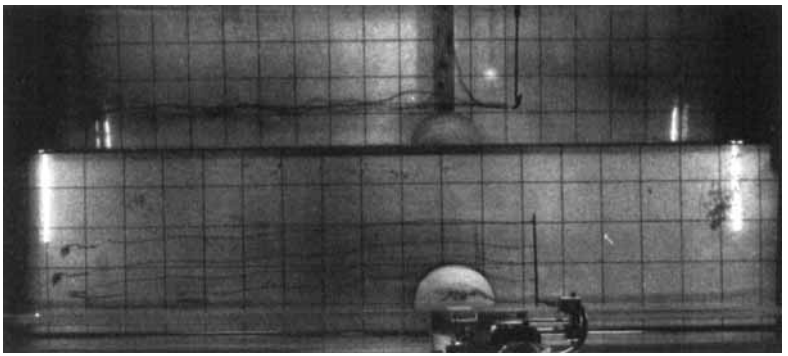

3(b)

FIGURE 3 Photographs of streamlines over the quarter-sphere for *clockwise* rotation and $\eta_0/H=\frac{1}{4}$. (a) Blocked flow with $Ro=0.03$, $E=9\times10^{-6}$; (b) Flow with no stagnation point and showing inertial lee waves at $Ro=0.11$, $E=9\times10^{-6}$. Dye lines originate at the height of the top of the obstacle and grid lines on the bottom of the channel are 5 cm apart.

At towing speeds intermediate to those of Figure 3 there is a slow transition between the two regimes described above, with the stagnation point moving further towards the downstream side of the obstacle and the blocked region decreasing in area as the towing speed is increased. For towing speeds above a critical value no blocking could be seen and streamlines pass almost directly over the

obstacle. Similar flow regimes were observed for the flow over the vertical half-cylinder and the elongated, ridge-like obstacle. The transition between the blocked and unblocked flows could be seen more clearly for the half-cylinder because, as a result of the flat top of this obstacle, the stagnation point shifts all the way to the rear of the obstacle before it disappears with increasing Rossby number.

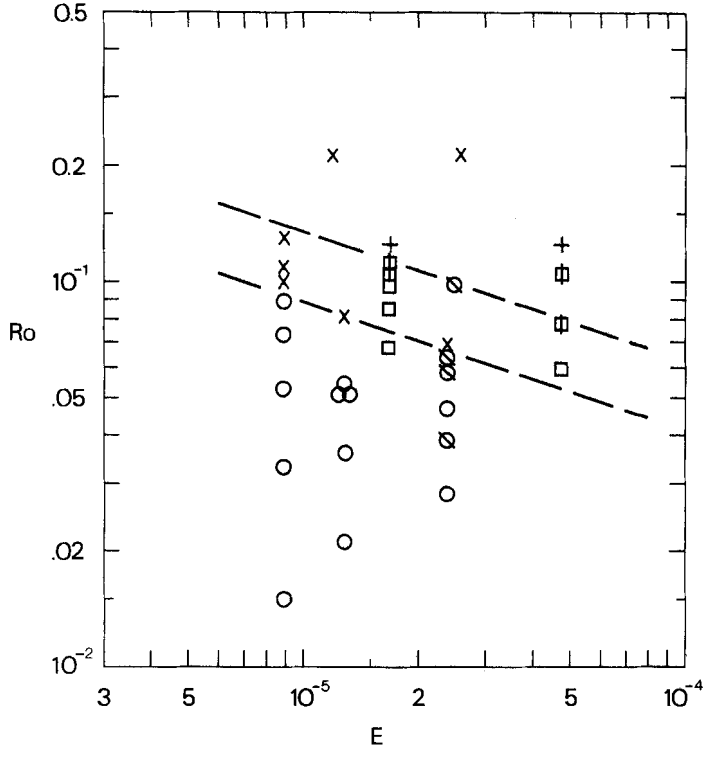


4(a)

On Figures 4(a) and (b) the flows over the quarter-sphere and vertical half-cylinder for obstacle depths $\eta_0/H=\frac{1}{4}$ and $\eta_0/H=\frac{1}{2}$, respectively, are classified according to whether or not a stagnation point appeared in the flow and plotted as a function of the Ekman and Rossby numbers. For $\eta_0/H=\frac{1}{4}$ [Figure 4(a)] the maximum Rossby number at which blocking occurs is approximately 30% lower for the spherical surface than for the sharp-edged and flat-

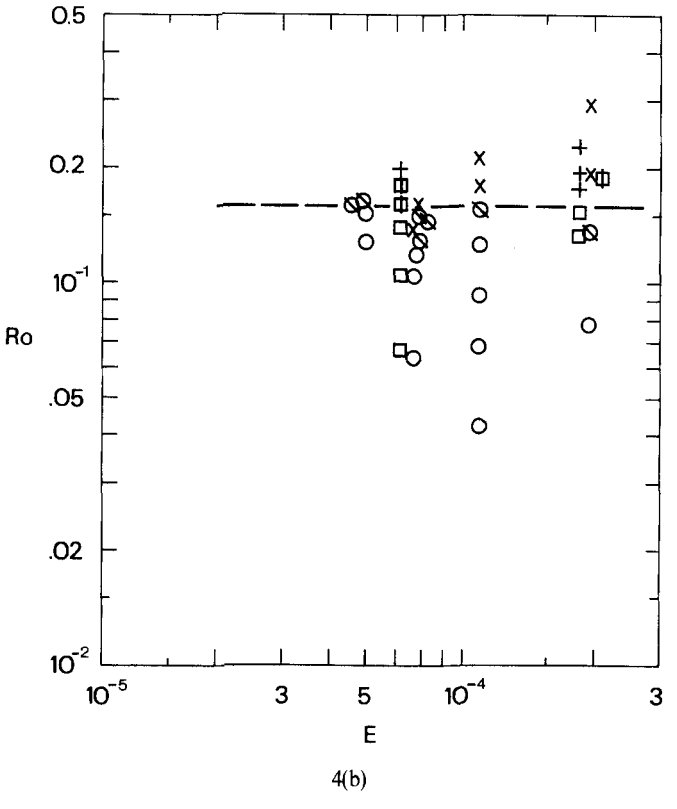


FIGURE 4 Classification of the flow for *clockwise* rotation and (a) $\eta_0/H=\frac{1}{4}$, (b) $\eta_0/H=\frac{1}{2}$. Symbols indicate flow with (○) or without (×) a stagnation point over the quarter-sphere and with (□) or without (+) a stagnation point over the vertical half-cylinder. ⃠ and ⊞ indicate flows with a doubtful classification. Lines show the approximate critical conditions for blocking. The upper line in (a) is for the half-cylinder, the lower for the quarter-sphere and both have slope $-\frac{1}{3}$. Note the different abscissa ranges for (a) and (b).

topped cylinder. Despite the uncertainty in deciding whether or not a stagnation point existed, the critical Rossby number is found to decrease slowly with increasing Ekman number: $Ro \sim E^{-1/3}$ satisfies the data for both obstacles. For the larger dimensionless obstacle depth, $\eta_0/H=\frac{1}{2}$ [Figure 4(b)], the critical Rossby numbers are significantly larger. Although the observations were taken at

generally larger Ekman numbers due to the smaller fluid depth, in the region where the data overlaps at $E \sim 5 \times 10^{-5}$ it can be seen that the critical value $Ro_c$ is a factor of two to three greater for $\eta_0/H = \frac{1}{2}$ than for $\eta_0/H = \frac{1}{4}$. At the same time there appears to be little difference between the conditions for stagnation over the two obstacles, and the critical Rossby number is now almost independent of Ekman number. Since a fluid column would have to compress and stretch by a much larger fraction in order to move over the larger obstacle there is less scope for Ekman friction to prevent blocking and a stagnation point is visible for $Ro < 0.16 \pm 0.02$.



### 4.2. Flow over submerged obstacles for anticlockwise rotation

When the direction of rotation is anticlockwise (positive), the wall again being on the left-hand side of the flow, the behaviour of the flow is very different to that for clockwise rotation. In this case there are at least three distinct flow regimes and on Figure 5 we show photographs of the streamlines over the quarter-sphere with $\eta_0/H = \frac{1}{4}$ are at least three distinct flow regimes and on Figure 5 (pages 16 and 17) we show photographs of the streamlines over the quarter-sphere with $\eta_0/H = \frac{1}{4}$ at four values of the towing speed but otherwise similar conditions. The most immediate feature of the flow is that the topography has a large downstream influence at all of the conditions attained. At the two lowest speeds shown on page 16 [Figures 5(a, b)] where the Rossby numbers are significantly less than $10^{-1}$, the downstream influence takes the form of a long wake that extends a large distance downstream along the wall. The flow in these cases is clearly blocked in the sense that there is a stagnation point (for an observer in a reference frame fixed in the obstacle) against the wall somewhere over the obstacle. Streamlines originating upstream curve to their right (away from the wall) as they approach the obstacle and the fluid then turns back to its left near the outer edge of the obstacle. However, instead of returning to the wall, the flow "separates" from an imaginary surface extending vertically throughout the depth of the fluid. By placing the dye injection at different depths and repeating the experiment it was found that the horizontal pattern of the streamlines is largely independent of depth (at least at heights above the maximum height

of the topography), although the vertical excursions of the dye lines near the obstacle are greater for lines originating closer to the bottom.

For very small Rossby numbers such as that of Figure 5(a) shown on page 16, where $Ro=0.02$, the large blocked region can be significantly wider than the obstacle itself and extends downstream through the full length of the channel. Within this region there is a slow recirculation that takes fluid from far *downstream* along the wall toward the obstacle (proving the presence of a stagnation point at the wall) and then back downstream near the outer edge of the wake. Note that, in the laboratory system, the fluid upstream is stationary relative to the wall and so there will be very little relative velocity between the wall and the fluid outside the wake. Thus there is very little net horizontal shear across the blocked region to drive the recirculation. The recirculating motion may be due entirely to the finite length of the tank, which requires that fluid be drawn into the wake at a finite distance downstream. If the fluid had a velocity $V$ relative to both the obstacle and the wall (i.e. if the fluid was moving and the wall and obstacle were stationary) there would be a large shear across the blocked region that could drive a more vigorous recirculation.

At larger towing velocities such as that of the flow in Figure 5(b) shown on page 16, where $Ro=0.06$, the large downstream blocked region is unstable. Small amplitude waves can be seen on the outer edge of the wake immediately behind the obstacle and, as they are advected downstream, these grow and roll-up into cyclonic eddies. Thus eddies are seen to roll-up some distance downstream from the obstacle. These eddies lie within the shear layer at the edge of the wake and sometimes have length scales only a fraction of the width of the wake. At still larger Rossby numbers it is no longer clear that eddies in the wake are associated with the shear layer downstream. Instead, as is the case for the flow shown in Figure 5(c) shown on page 16, where $Ro=0.1$, large cyclonic eddies are shed immediately at the obstacle. More streamlines now pass over the topography so that, along with a greater likelihood that the flow will separate from the obstacle surface itself, the increased stretching and bending of vortex lines due to the flow over the topography may intensify cyclonic vorticity throughout the fluid depth. The flow is unsteady, with the eddies tending to break up the wake as they are advected

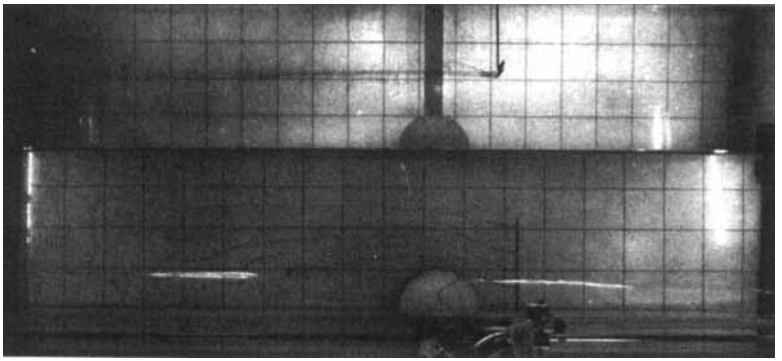

5(a)

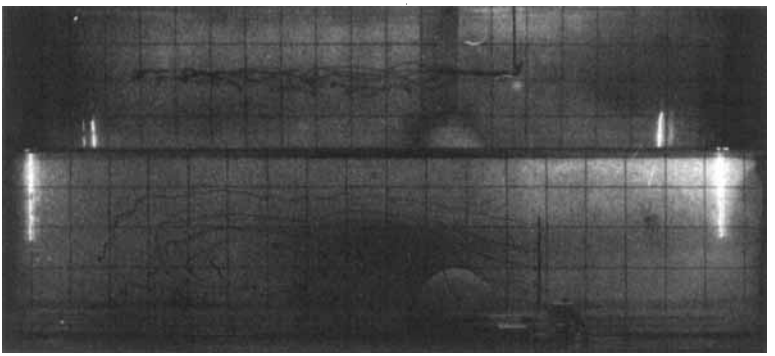

5(b)

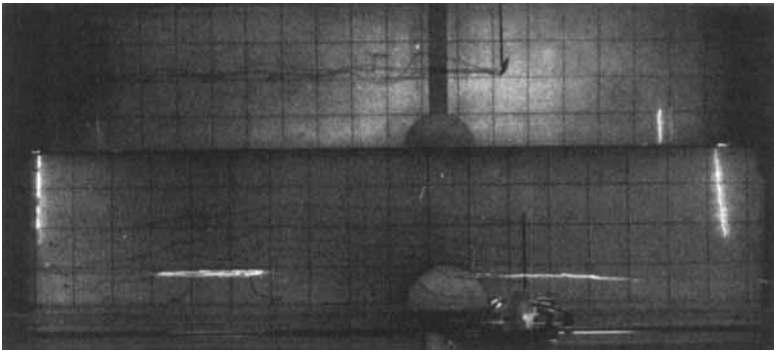

5(c)

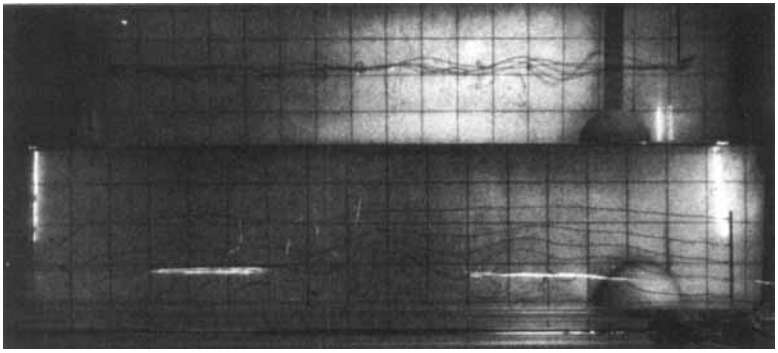

5(d)

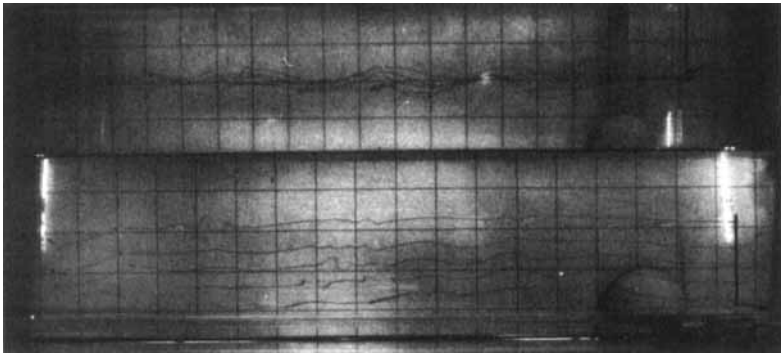

5(e)

FIGURE 5 Photographs of streamlines in the flow over the quarter-sphere for *anticlockwise* rotation and $\eta_0/H=\frac{1}{4}$, showing (a) a large stable blocked region at $Ro=0.02$, $E=13\times10^{-6}$; (b) formation of eddies from unstable waves on the blocked region at $Ro=0.06$, $E=9\times10^{-6}$; (c) shedding of cyclonic eddies along with blocking at $Ro=0.1$, $E=13\times10^{-6}$; (d) cyclonic eddies well behind the obstacle at $Ro=0.14$ and $E=13\times10^{-6}$; and (e) standing inertial lee waves at $Ro=0.2$, $E=24\times10^{-6}$. Dyed streamlines originate at mid-depth (or two obstacle heights above the bottom) and the side view is at the top of each photograph.

downstream. Far downstream the flow consists entirely of uniformly spaced cyclonic eddies near the wall and a noticeable feature is that the eddy spacing is significantly larger than the scale of an individual eddy [Figure 5(d)] shown on page 17.

At large Rossby numbers the recirculating wake and stagnation point disappear at heights above the maximum height of the obstacle, and the disturbance created by the topography is dominated by a system of inertial lee waves. Figure 5(e) on page 17 shows an example for $\eta_0/H=\frac{1}{4}$ and $Ro=0.2$. Note that these conditions are similar to those of the flow in Figure 3(b), where the rotation was clockwise, but that the waves appear to be a larger amplitude in the case of anticlockwise rotation. The horizontal view in Figure 5(e) shows that the streamlines undergo large vertical as well as horizontal excursions in the waves, the amplitude decreasing away from the wall and with distance downstream. An injection of dye near the bottom immediately behind the obstacle under these conditions reveals that a three-dimensional separation bubble exists, but that this is confined to within the height and width of the obstacle and extends only about one obstacle width downstream.

Flow regimes similar to those illustrated on Figure 5 and described above were observed when the fluid depth was decreased to give $\eta_0/H=\frac{1}{2}$. The only significant qualitative difference appeared at large Rossby numbers where, with the larger obstacle height, the inertial lee waves attained such large amplitudes that they appeared to break down near the wall, producing cyclonic eddies. Such eddies were formed several wavelengths downstream from the obstacle in many cases and might have been due to a velocity shear associated with a flow along the wall behind the obstacle. However, those conditions at which eddies formed from "breaking" lee waves could not be clearly separated from those at which the eddies were shed by the topography. The breakdown of lee waves at the wall was not observed when $\eta_0/H=\frac{1}{4}$, possibly because all experiments then used a smaller Rossby number, but also because the wave amplitude at a given Rossby number is larger for the larger obstacle height.

All of the observations of flow over the quarter-sphere and vertical half-cylinder for anticlockwise rotation (the wall being on the left of the flow) were classified as belonging to one of three flow regimes and are plotted on Figure 6 as a function of the Ekman and Rossby numbers. The three regimes are: (i) flow involving a stable blocked

region downstream; (ii) flow in which there is a stagnation point over the obstacle and a definite wake, but which contains cyclonic eddies; and (iii) flow in which the dominant disturbance to uniform flow (at levels above the top of the obstacle) is a system of standing lee waves. Stable blocked regions are found at small Rossby numbers and large Ekman numbers while a reduction of the influence of either viscosity or Coriolis forces tends to de-stabilize the shear layer at the edge of the wake. The blocked region also tends to be much more unstable for the larger obstacle height [compare Figures 6(a) and (b)]. The conditions for stable wakes are well described by the relations

$$Ro\,E^{-5/4} < 4.5 \times 10^4, \quad \eta_0/H = \tfrac{1}{4}, \tag{4.1}$$

and

$$Ro\,E^{-5/4} < 1.1 \times 10^4, \quad \eta_0/H = \tfrac{1}{2}. \tag{4.2}$$

These boundaries are shown on Figures 6(a) and (b), respectively, and do not appear to depend strongly upon the shape differences between the two obstacles.

The conditions at which the stagnation point and the wake disappear are dependent primarily on the dimensionless obstacle height. When $\eta_0/H = \frac{1}{4}$ [Figure 6(a)] there is a weak dependence on the Ekman number and no blocking was visible for

$$Ro > 7.0 \times 10^{-3}\,E^{-1/3}. \tag{4.3}$$

When $\eta_0/H = \frac{1}{2}$, no blocking was seen for

$$Ro > 0.4, \tag{4.4}$$

although there is insufficient data to be certain that this criterion is independent of Ekman number.

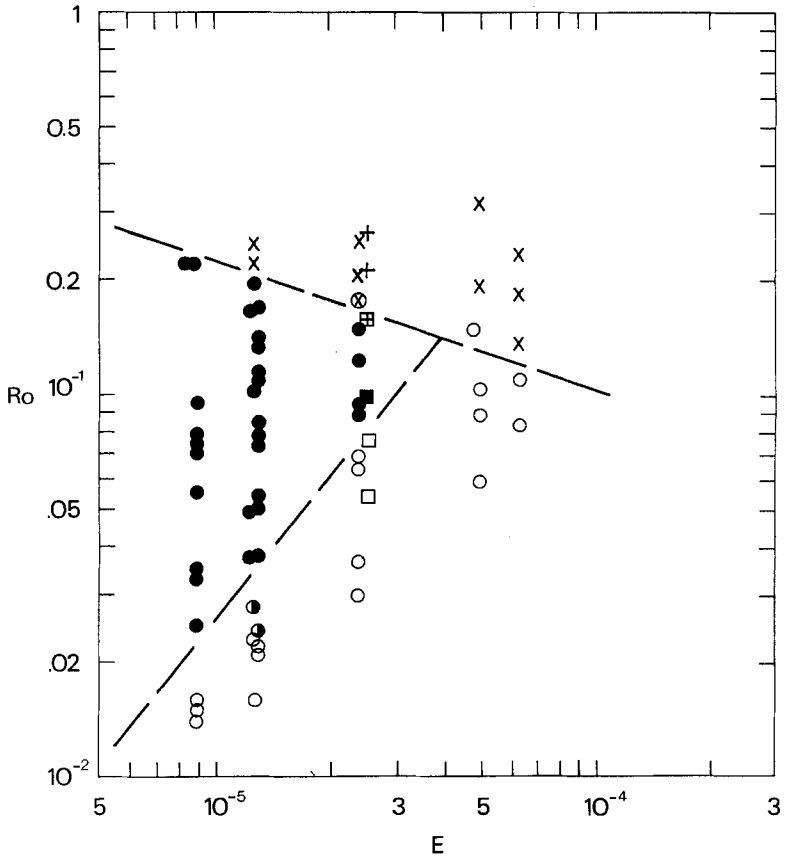


6(a)

### 4.3. Flow about a submerged ridge

In order to increase the rate of variation, in the downstream direction, of the obstacle width we used the triangular ridge with $l/d = l/\eta_0 = 3$.

With this elongated obstacle we have concentrated upon the nature of the flow for anticlockwise rotation and find three flow regimes that are qualitatively similar to those observed for the quarter-sphere: a large and almost stagnant region developed

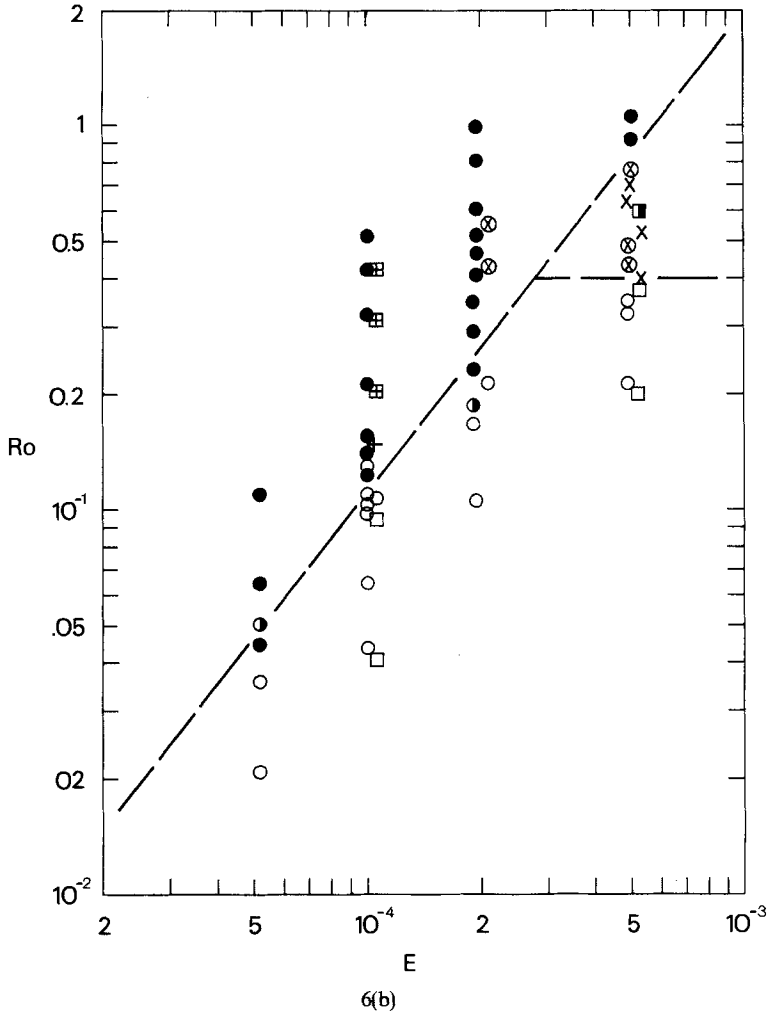


FIGURE 6 Classification of flows over the quarter-sphere and half-cylinder for *anticlockwise* rotation with (a) $\eta_0/H=\frac{1}{4}$ and (b) $\eta_0/H=\frac{1}{2}$. For the quarter-sphere there is a stable blocked region downstream (○), blocking with cyclonic eddies in the wake (●), or no blocking but a system of lee waves (×). Symbols ◑, ⊗ indicate uncertain classification. For the half-cylinder the same regimes are indicated by □, ■ and +, respectively, with ◨ and ⊞ as uncertain cases. Broken lines show the position of transitions between flow regimes (see Eqs. 4.1–4.4).

downstream of the ridge at very small towing speeds; eddies appeared in the wake at intermediate towing speeds; and the blocked region was replaced by a system of lee waves at large speeds. These observations are summarised on Figure 7(a) and (b) for two fluid

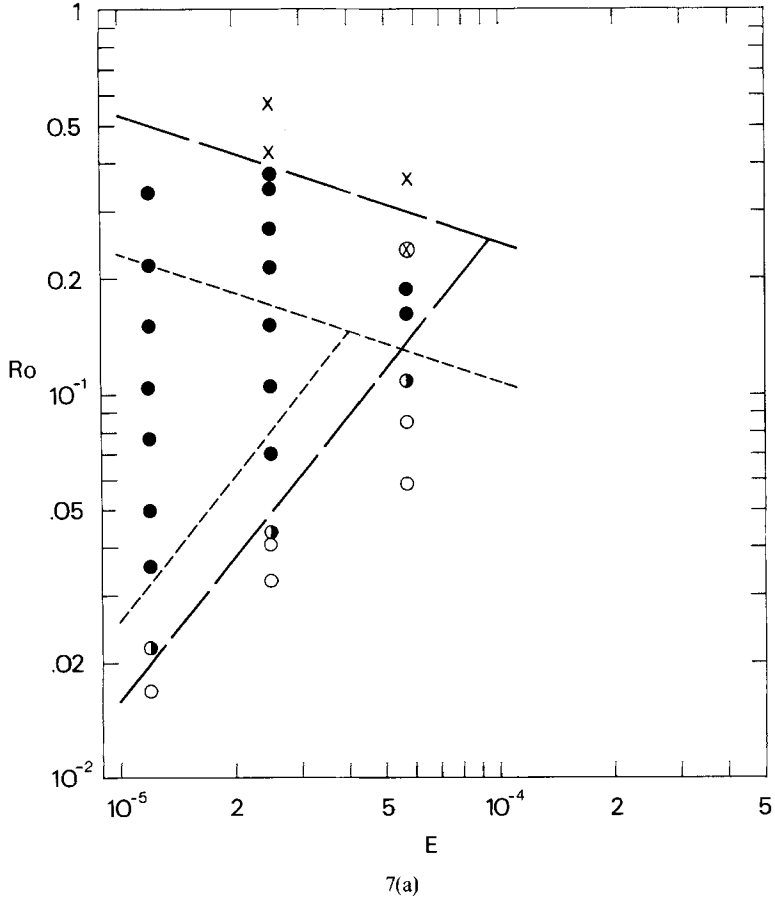


7(a)

depths giving $\eta_0/H=\frac{1}{4}$ and $\eta_0/H=\frac{1}{2}$, respectively. By comparing these data with those on Figure 6 for the other obstacles, we see that an unsteady wake with cyclonic eddies persists behind the "ridge" up to Rossby numbers close to twice as large as the critical Rossby numbers for the other obstacles. Furthermore, the transition from a stable blocked region to a wake containing cyclonic eddies occurs at

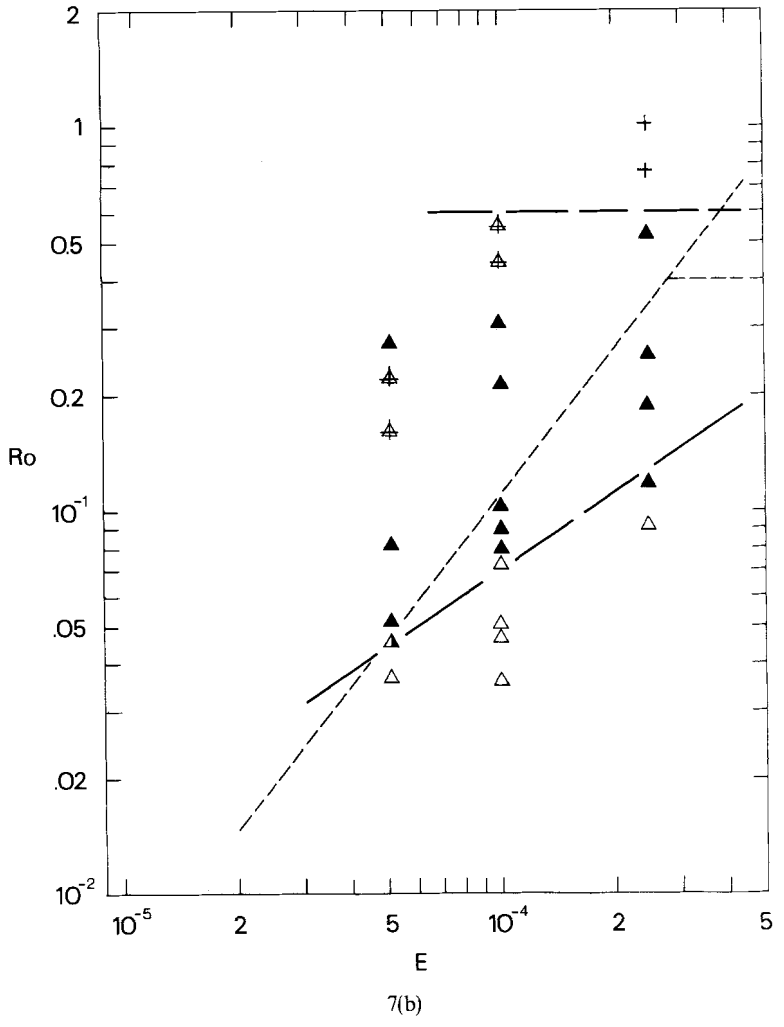


FIGURE 7 Classifications of flows over the ridge-like obstacle (with $l/d=3$) for *anticlockwise* rotation when (a) $\eta_0/H=\frac{1}{4}$ ($l/H=\frac{3}{4}$) and (b) $\eta_0/H=\frac{1}{2}$ ($l/H=\frac{3}{2}$). Symbols indicate the three flow regimes as in Figure 6 (circles for $\eta_0/H=\frac{1}{4}$, triangles for $\eta_0/H=\frac{1}{2}$). Broken lines indicate the transitions. In each case the lower line is the best fit to the data using a slope $\frac{5}{4}$ in (a) and a slope $\frac{2}{3}$ in (b). For comparison, the dotted lines are the boundaries from Figure 6 and indicate the conditions at which the corresponding transitions were observed behind the quarter-sphere.

Rossby numbers approximately one half those for the corresponding transition on Figure 6. The variation with obstacle height $\eta_0/H$ of the nature of the flow over the "ridge", on the other hand, is very similar to that observed with the more slowly varying obstacles.

Qualitative observations suggest that eddies only appeared in the flow over the ridge-like obstacle when some streamlines passed over the crest of the ridge, while the blocked region was stable when all streamlines flowed around the end of the ridge. The eddies also seemed to form immediately behind the obstacle and did not appear to be the products of unstable waves on the shear layer.



### 4.4. Flow around a half-cylinder extending throughout the fluid depth

Although the flow about submerged obstacles was found to be independent of depth at levels above the top of the obstacle when the Rossby number was small ($<10^{-1}$) and still qualitatively independent of depth at larger Rossby numbers, the three-dimensional nature of the topography is essential for the production of inertial waves and may also be an important influence on the eddy-shedding mechanisms at intermediate Rossby numbers. In order to remove the influence of flow over the topography, the fluid depth was reduced to a value just slightly less than the height (5.0 cm) of the vertical half-cylinder, so that the cylinder formed a two-dimensional obstacle against the channel wall.

On Figure 8 are shown photographs of the flow around the vertical half-cylinder that extends throughout the fluid depth ($\eta_0/H=1$). For clockwise rotation [Figure 8(a)] and all towing speeds available, the streamlines originating upstream are simply deflected around the obstacle, with little vertical displacement, and return to their initial distance from the wall downstream of the cylinder. Apart from a confined separation region no downstream wake or wave motions were detected at all Rossby numbers. When the rotation is anticlockwise, on the other hand, the streamlines always separate from the obstacle and for very small Rossby numbers ($Ro \leqq 0.03$) they outline a large, slowly recirculating wake or blocked region. The length of this blocked region decreases with increasing $Ro$ and for $Ro \approx 0.1$ the flow [Figure 8(b)] is very similar to that for clockwise rotation. For large Rossby numbers, on the

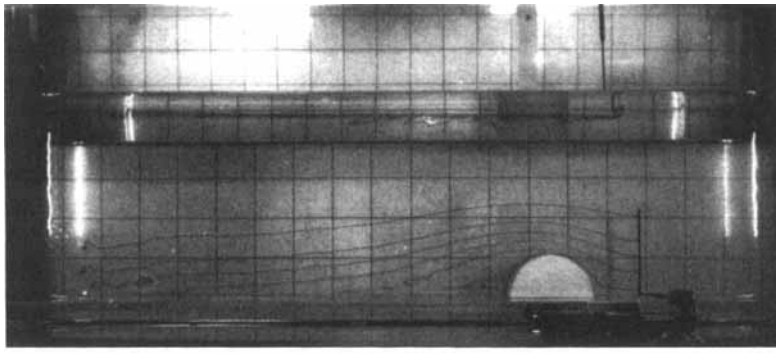

8(a)

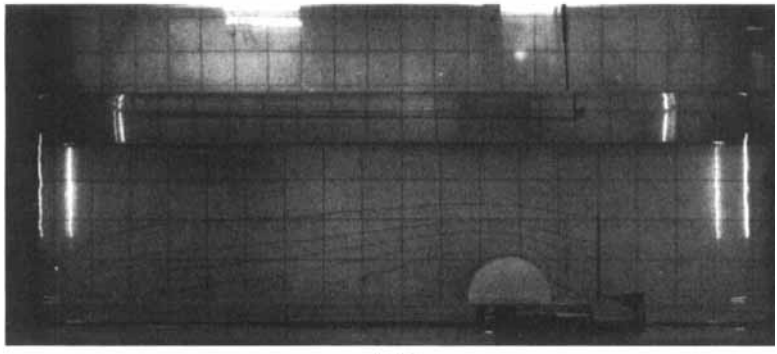

8(b)

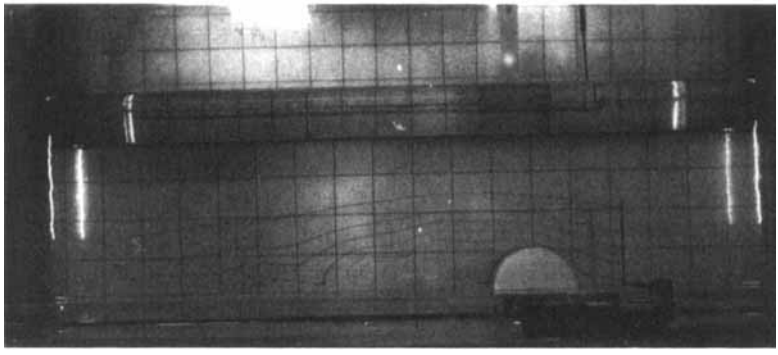

8(c)

FIGURE 8 Photographs of flow around the half-cylinder against the wall and extending throughout the fluid depth: (a) clockwise rotation, $Ro = 0.09$, $E = 280 \times 10^{-6}$; (b) anticlockwise rotation, $Ro = 0.1$, $E = 280 \times 10^{-6}$; (c) anticlockwise rotation, $Ro = 0.2$, $E = 280 \times 10^{-6}$.

other hand, the wake is present but contains cyclonic eddies [Figure 8(c)] shown on page 25. For the smaller Rossby numbers at which eddies were observed, the eddies appeared to form from unstable waves within the shear layer at the outer edge of the wake. However, as was the case for flow over the same obstacle with $\eta_0/H = \frac{1}{4}, \frac{1}{2}$, the eddy formation mechanism may again be different at larger Rossby numbers, where the eddies appeared to be shed directly from the obstacle itself.

The observations for anticlockwise rotation are summarised on Figure 9, where we again have not been able to clearly separate the two possible mechanisms of eddy formation. The broken line shows roughly those conditions at which eddies begin to appear in the wake and is the line

$$Ro = 39E^{2/3}. \tag{4.5}$$

Note that this line is identical to a boundary for an *isolated* vertical cylinder (Boyer, 1970), the transition in that case being from a flow with an unsteady system of attached eddies to one in which eddies were shed from the right-hand side of the cylinder (looking downstream). This transition for the isolated cylinder occurs at Rossby numbers only slightly greater than the transition from a steady wake involving a double eddy. Thus the presence of the wall on the left-hand side of the flow (with anticlockwise rotation) appears to have little effect on the conditions at which eddy shedding occurs. Furthermore, although large blocked regions are not found behind isolated cylinders at small Rossby numbers, Boyer found that the transition from fully attached flow to flow with a single attached eddy lies at Rossby numbers well below those of all the present experiments and therefore we do not expect to observe fully attached flow.

## 5. DISCUSSION AND CONCLUSIONS

The presence of a vertical wall immediately adjacent to bottom topography in a rotating system has a marked influence upon the flow over the topography and the behaviour of the flow depends

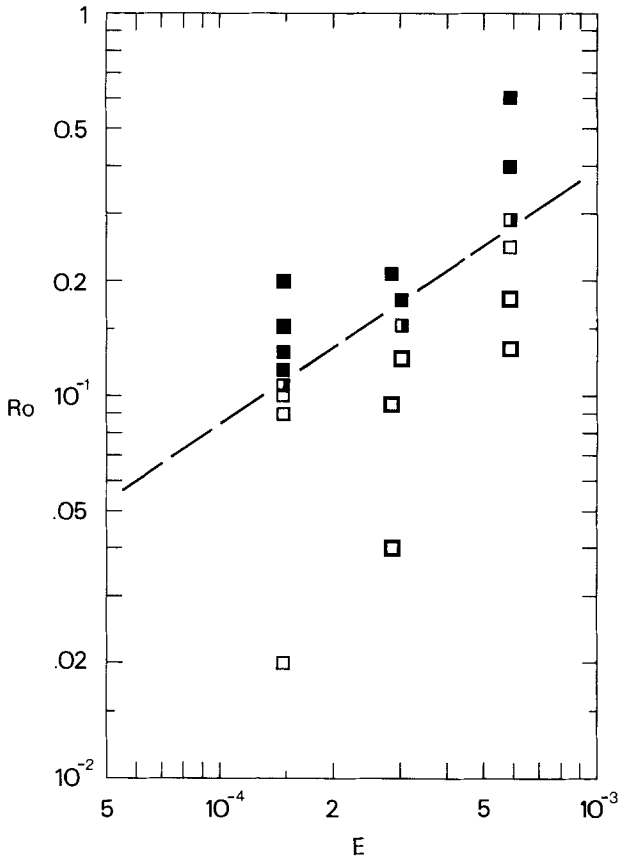


FIGURE 9 Classification of the flows around the vertical half-cylinder with $\eta_0/H = 1$ and *anticlockwise* rotation: □—flow with a stable blocked region downstream; ■—flow with cyclonic eddies in the wake; ◨—uncertain classification. The broken line (4.5) has slope $\frac{2}{3}$.

strongly upon the direction of rotation of the system. Although the experiments were all carried out by towing an obstacle along the right-hand wall (looking in the direction of motion of the obstacle) of a wide channel which was rotated in both directions, the conditions can be transformed into those viewed by an observer who is fixed in a system rotating anticlockwise, moving with the obstacle and looking in the direction of the relative fluid velocity $V$. Thus the

flow in the experiments with clockwise rotation is equivalent to flow with a wall on its right-hand side in a system rotating anticlockwise, while the flow in the experiments with anticlockwise rotation has the wall on its left.

When the wall is on the right-hand side of the flow (with positive rotation), two flow regimes can be identified. At small Rossby numbers there is a stagnation point and a blocked region above the obstacle similar to that which occurs over an isolated obstacle, while at large Rossby numbers there is no blocking and only a system of standing inertial lee waves downstream of the topography. At very low Rossby numbers the topography has no significant downstream influence. The critical Rossby number below which blocking occurs increases slowly as the influence of friction (the Ekman number) decreases. A value for this critical Rossby number is predicted by the inviscid analysis for slowly varying obstacles: for the quarter-sphere (2.10) gives the critical value $Ro_c = \frac{1}{4}\pi(\eta_0/H)$, which becomes $Ro_c \approx 0.196$ for the obstacle height $\eta_0/H = \frac{1}{4}$, and $Ro_c \approx 0.393$ for $\eta_0/H = \frac{1}{2}$. For the half-cylinder the critical value is simply $Ro_c = \eta_0/H$ ($= \frac{1}{4}$ and $\frac{1}{2}$). Comparison with the data on Figures 4(a) and (b) shows that both the qualitative dependence on obstacle height and on the different cross-sectional areas of the spherical and cylindrical obstacles are well predicted. On the other hand, the observed critical Rossby numbers, at the Ekman numbers used in the laboratory, are a factor of more than two smaller than those predicted. This difference can be attributed to the effects of Ekman friction and to the finite downstream length scale of the obstacles.

When the wall lies on the left of the flow (again with positive rotation) the behaviour is markedly different. At low Rossby numbers there is again a stagnation point over the obstacle, but this time the topography has a very large downstream influence in the form of a slowly recirculating wake. At the very lowest Rossby numbers used (see Figure 6) the downstream extent of the wake appears to be only limited by the finite length of the channel. As the Rossby number is increased cyclonic eddies appear in the wake, apparently generated by two different mechanisms: for the flow about the quarter-sphere and vertical half-cylinder small eddies are first produced by rolling-up of unstable waves on the shear layer at the outer edge of the blocked region, then at larger Rossby numbers the attached wake gives way to a train of large eddies that are

generated immediately behind the obstacle. These two regimes could not be clearly separated in parameter space and so they have been included into a single flow regime. At very large Rossby numbers the unsteady eddy-shedding regime is replaced by a very different regime in which the only significant downstream influence is a system of large amplitude lee waves similar to those observed with the wall on the right. No fully attached flow was observed and we suggest that the large blocked region downstream will occur on all Rossby numbers below those attained in these experiments.

The appearance of a stagnation point on the left-hand wall is not predicted by the nonlinear analysis for slowly varying obstacles (Section 2.2), nor by the linearised analysis for more general topography (Huppert and Stern, 1974b). It is therefore likely to be a nonlinear phenomenon associated with the finite downstream length scale of the topography. This would be consistent with our observations of a large, slowly recirculating wake against the left-hand wall downstream of a two-dimensional half-cylinder that extends throughout the fluid depth. In that case, separation of the flow from the cylinder requires nonlinear inertial effects, just as in a non-rotating flow. The conclusion that blocking near the left-hand wall is due to the rapid downstream variation of obstacle width is also supported by our observations of flow over the elongated, ridge-like obstacle (Figure 7), which show that a stagnation point exists on the left-hand wall over the ridge at larger Rossby numbers (but the same $\eta_0/H$) than is the case for obstacles with equal width, length and height. Thus the critical Rossby number depends upon the ratio of obstacle height to obstacle width. It is also interesting to note that for each obstacle shape and each Ekman number investigated, the critical Rossby number for blocking in the presence of a wall on the left-hand side of the flow is larger than that for blocking in the presence of a wall on the right (with rotation anticlockwise).

The nature of the eddy generation mechanism in flow against a wall on the left has not been fully resolved and requires further study. In the flow about a quarter-sphere and vertical half-cylinder unstable waves roll-up to form eddies some distance downstream of the topography. These eddies lie within the shear layer at the edge of the blocked region and sometimes have length scales only a small fraction of the width of the wake. Hence the shear layer appears to be unstable despite the fact that the background vorticity $2\Omega$, which

has the same sign as the local relative vorticity $v_x$, should tend to stabilize the flow (Tritton and Davies, 1979). A similar formation of eddies has been observed downstream of an isolated vertical cylinder in a zonal flow with a $\beta$-effect (McCartney, 1975), despite the stabilizing tendency of the $\beta$-effect. It is, therefore, not unreasonable that a similar shear instability occurs in the present experiments which involve no $\beta$-effect in the direction perpendicular to the wall. (The small variation of fluid depth along the channel caused by centrifugal forces also has no obvious influence on the flows observed apart from a small variation of the position of the stagnation point that was sometimes detectable at the larger values of $\Omega$ as the obstacle moved along the channel.) No unstable waves were seen in the flow past the ridge-like obstacle, and this may have been due to a wider and therefore more stable shear layer.

Since the generation of eddies in the presence of a left-hand wall is found to be suppressed by viscosity, enhanced by increasing inertial forces and assisted by greater obstacle size, the Reynolds number $Re = Vl/\nu$ may be the most appropriate indicator of wake stability. The Reynolds number is independent of the Rossby and Ekman numbers but related to them by

$$Re \equiv \frac{Ro}{E}\left(\frac{l}{H}\right)^2. \tag{5.1}$$

Thus lines of unit slope on each Rossby/Ekman number diagram represent constant Reynolds numbers. The data for flows over the quarter-sphere and vertical half-cylinder with $\eta_0/H = \frac{1}{4}$ [Figure 6(a)] are presented again on Figure 10, this time in terms of the Reynolds and Rossby numbers of the flow. Instability of the wake occurs at a value of the Reynolds number that has a weak but significant dependence upon the Rossby number (the same dependence being found for $\eta_0/H = \frac{1}{2}$), with increasing rotation decreasing the critical Reynolds number $Re_c$. The stability boundary (4.1) now becomes, using (5.1) and $l/H = \frac{1}{4}$,

$$Re_c \approx 326\, Ro^{1/5}. \tag{5.2}$$

Similarly, blocking occurs at $Re > 5 \times 10^5\, Ro^4$.

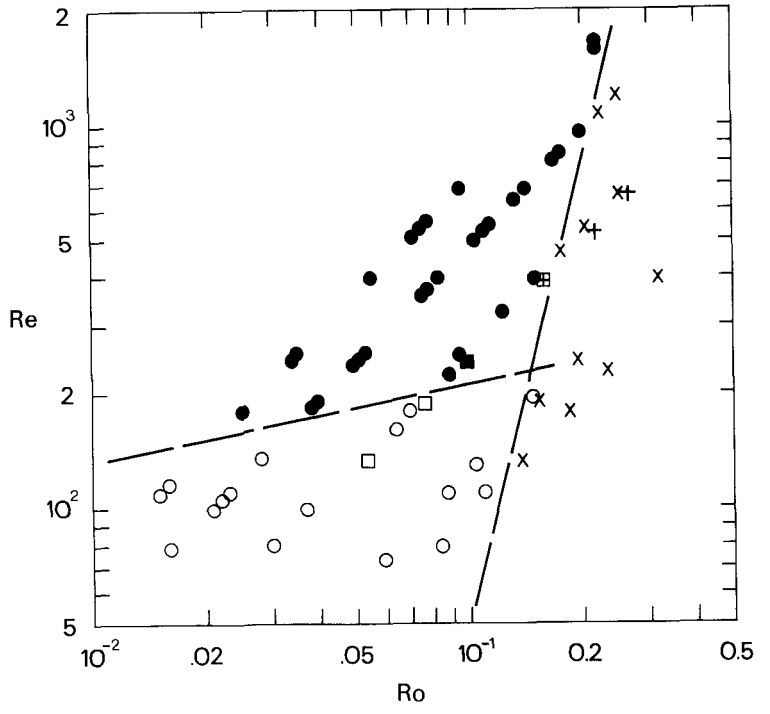


FIGURE 10 The data of Figure 6(a) presented again on a Reynolds number/Rossby number diagram, showing the Reynolds numbers of the laboratory flows over both the quarter-sphere and half-cylinder for $\eta_0/H = \frac{1}{4}$ and anticlockwise rotation. Symbols are as on Figure 6. The lines [see (5.2)] have slopes $\frac{1}{5}$ and 4.

The Rossby number dependence in (5.2) is in contrast to that found for the onset of instability in the wake behind a half-cylinder that extends throughout the fluid depth. In that case the boundary is (4.5), which becomes

$$Re_c \approx 243\, Ro^{-1/2}, \tag{5.3}$$

a result which is consistent with that for the onset of eddy shedding from an *isolated* cylinder (Boyer, 1970). The difference between (5.2) and (5.3) is presumably due to the presence or absence of a vertical solid surface throughout the fluid depth from which separation and eddy shedding can occur. The experiments indicate that the

generation of eddies immediately downstream of the submerged obstacles is instead closely associated with a flow of fluid over (rather than around) the topography. Under suitable conditions, then, the shear layer may become unstable before shedding occurs. With this in mind we recall that the slope of the stability boundary for the flow over the "ridge" with $\eta_0/H=\frac{1}{2}$ [Figure 7(b)] is most consistent with that of the boundary for the two-dimensional cylinder extending throughout the depth of the fluid, and that the boundary is at smaller Rossby numbers than those for the other obstacles at the same value of $\eta_0/H$. Because the "ridge" has a smaller ratio of height to width than the quarter-sphere and vertical cylinder there is flow over the crest of the ridge, and associated eddy generation, at smaller Rossby numbers.

More needs to be said about the dependence upon obstacle size of the behaviour on Figures 6 and 10. Although we have used only two submerged obstacle heights, the two empirical stability boundaries (4.1) and (4.3) for $\eta_0/H=\frac{1}{4}$ and $\eta_0/H=\frac{1}{2}$, respectively, together suggest that the wake is stable when

$$Ro<2.78\times10^3\,E^{5/4}(\eta_0/H)^{-2}. \tag{5.4}$$

Since this relation is obtained for obstacles with $l/H=\eta_0/H$, (5.1) and (5.4) can be combined to give a tentative dependence upon the obstacle size of the critical Reynolds number:

$$Re_c\approx 569\,Ro^{1/5}\left(\frac{l}{H}\right)^{2/5}. \tag{5.5}$$

However, caution is necessary in applying the laboratory results to nature since the ratios of topographic width to fluid depth of interest in coastal flows ($l/H\sim10^2$) are typically two to three orders of magnitude larger than those used in the laboratory. This means that the laboratory Reynolds numbers are so small that the flow is unlikely to be similar in all respects to that at oceanic scales.

Finally, there is much yet to be learned about the large amplitude inertial lee waves that have been observed, and in particular about the resulting drag exerted on the flow by the coastal topography. Similar waves generated by isolated obstacles have been studied theoretically by Cheng (1977) and Stewartson and Cheng (1979), but little attention has been paid to them in laboratory experiments.

## Acknowledgements

This work was supported by a grant from the Natural Environment Research Council. We are grateful to D. Cheesley, D. Lipman and J. Sharpe for the construction of the towing tank.

## References

Baines, P. G. and Davies, P. A., in "Orographic effects in planetary flows," GARP publication No. 23, World Meteorological Organisation (1980).

Boyer, D. L., "Flow past a right circular cylinder in a rotating frame," *J. Basic Eng. Am. Soc. Mech. Eng. D* **92,** 430–436 (1970).

Boyer, D. L., "Rotating flow over long shallow ridges," *Geophys. Fluid Dyn.* **2,** 165–184 (1971a).

Boyer, D. L., "Rotating flow over a step," *J. Fluid Mech.* **50,** 675–687 (1971b).

Boyer, D. L. and Davies, P. A., "Flow past a circular cylinder on a $\beta$-plane," *Phil. Trans. Roy. Soc. Lond. A* **306,** 533–556 (1982).

Cheng, H. K., "On inertial wave and flow structure at low Rossby number," *Z. Angew. Math. Phys.* **28,** 753–769 (1977).

Davies, P. A., "Experiments on Taylor columns in rotating stratified fluids," *J. Fluid Mech.* **54,** 691–717 (1972).

Hide, R. and Ibbetson, A., "An experimental study of Taylor columns," *Icarus* **5,** 279–290 (1966).

Huppert, H. E., "Some remarks on the initiation of inertial Taylor columns," *J. Fluid Mech.* **67,** 397–412 (1975).

Huppert, H. E. and Stern, M. E., "The effect of side walls on homogeneous rotating flow over two-dimensional obstacles," *J. Fluid Mech.* **62,** 417–436 (1974a).

Huppert, H. E. and Stern, M. E., "Ageostrophic effects in rotating stratified flow," *J. Fluid Mech.* **62,** 369–385 (1974b).

Ingersoll, A. P., "Inertial Taylor columns and Jupiter's Great Red Spot," *J. Atmos. Sci.* **26,** 744–752 (1969).

McCartney, M. S., "Inertial Taylor columns on a Beta plane," *J. Fluid Mech.* **68,** 71–95 (1975).

Maxworthy, T., "Topographic effects in rapidly rotating fluids: Flow over a transverse ridge," *Z. Angew. Math. Phys.* **28,** 853–864 (1977).

Stewartson, K. and Cheng, H. K., "On the structure of inertial waves produced by an obstacle in a deep rotating container," *J. Fluid Mech.* **98,** 415–433 (1979).

Tritton, D. J. and Davies, P. A., "Instabilities in geophysical fluid dynamics," in *Topics in Applied Physics* **45,** 229–270 (1979).

Vaziri, A. and Boyer, D. L., "Rotating flow over shallow topographics," *J. Fluid Mech.* **50,** 79–95 (1971).